SIGNATURES OF SYMMETRY-PROTECTED TOPOLOGY IN ENTANGLEMENT ENTROPY FOR ONE-DIMENSIONAL SYSTEMS

A Thesis submitted for the completion of
requirements for the degree of

Bachelor of Science
(Research)

by

Aman Anand
11-01-00-10-91-17-1-14807
Undergraduate Programme
Indian Institute of Science

Under the supervision of

Prof. Sumilan Banerjee
Department of Physics, Indian Institute of Science

Acknowledgement

I would like to express my gratitude towards my guide Prof· Sumilan Banerjee for taking me under his care and patiently supporting me throughout the journey. I also thank my mentors Surajit Bera and Jagganath Sutradhar, for helping me all along. I would also like to thank my friends for helping me in my tough times and motivating me to work hard. My heartfelt gratitude towards my parents for always providing me with their love and support. At last, I would like to thank KVPY and IISc for giving me the resources to do this project.

Abstract

The main goal of my project was to study- "How signatures of symmetry-protected topology (SPT) manifest in entanglement entropy". I studied this effect for the 1D SSH model, a non-interacting model and has a trivial and topological phase protected by chiral symmetry. I calculated the entanglement entropy using the correlation matrix. The entanglement entropy here follows the area law. Talking about entanglement entropy makes sense mostly for zero temperature ($T = 0$) where we have the ground state. However, I also calculated the von Neumann entropy for a subsystem for some time-evolving pure states, e.g., a density wave state. I found that the evolution of entanglement entropy with time is not significantly different for the two phases, i.e., topological and trivial. This is due to the fact that the initial pure states were very high energy states, and the signatures of topology can only be seen at low energies. I also looked into the effects of boundary conditions, disorder, and different initial pure states on the entanglement entropy.

Contents

1. Introduction

Starting from the 80's topology entered physics, and since then, topological physics has been exploding with new kinds of materials like topological insulators. The same goes for entanglement, which first garnered interest from the community, starting from the famous EPR paradox. Entanglement forms the basis of disparity between classical and quantum physics. It has wide-ranging applications from quantum information theory to quantum computation.

Entanglement measures have been used to identify topologically non-trivial features in higher dimensional many-body systems. Like for long-range entangled topological states, the von Neumann entropy with system size changes as $S(L) = \alpha L^{D-1} - \gamma + ...$ [**PhysRevLett.96.110404**] where the constant γ is a universal constant which depends on topological invariants. It has also been shown that the entanglement spectrum (Schmidt eigenvalues of many-body state) contains information about the topological properties [**PhysRevLett.101.010504**]. The entanglement entropy in the ground state obeys the area law, but for d=1, a distinction has to be made between the critical and non-critical ground states [**LAFLORENCIE20161**]. The area law is always obeyed for non-critical ground states having a finite correlation length [**Calabrese˙2004**, **Eisert˙2010**].

It has been shown [**PhysRevB.101.235155**] that for the SSH model that there are oscillations in entanglement entropy for odd and even subsystem sizes (see section 4.1), and the difference between those can be used to show the transition between topological and trivial phase for the ground state.

2. Basic Definitions

2.1 Entanglement

In a quantum many body systems with n-particles, the Hilbert space H is a tensor product of subsystem spaces given as $\mathrm{H} = \otimes_{l=1}^{n} H_l$. Then we can write a general state in H as

$$|\psi\rangle = \sum_{\mathbf{i}_n} c_{\mathbf{i}_n} |\mathbf{i}_n\rangle, \tag{2.1}$$

where $\mathbf{i}_n = i_1 i_2 ... i_n$ is a multi-index and and $|\mathbf{i}_n\rangle = |\mathbf{i}_1\rangle \otimes |\mathbf{i}_2\rangle \otimes ... \otimes |\mathbf{i}_n\rangle$. This state $|\psi\rangle$ in general cannot be written as a product state of individual subsystems, i.e. $|\psi\rangle \neq |\psi_1\rangle \otimes |\psi_2\rangle \otimes ... \otimes |\psi_n\rangle$ [**RevModPhys.81.865**]. That means in general we cannot think of a total system as product state of single state vectors. This is the idea of entanglement. It can be better understood with the below example for the Bell state:

$$|\psi\rangle = \frac{|10\rangle + |01\rangle}{\sqrt{2}} \neq (a_1|0\rangle + b_1|1\rangle) \otimes (a_2|0\rangle + b_2|1\rangle) \quad \forall\ a_1, b_1, a_2, b_2 \tag{2.2}$$

The states which can be written as product states are known as separable states. There is another recent definition of entanglement, which states-"Entangled states are the ones that cannot be simulated by classical correlations" [**Masanes˙2008**].

2.2 Entanglement measures

It is beneficial to measure the information stored in a quantum many-body state from the aspect of quantum computing. The need to measure also arises when one needs to understand how many states contribute to an entangled state. Thus, it is useful to introduce a measure for entanglement.

2.2.1 Schmidt Decomposition and Schmidt Rank

We think of a quantum system divided into two distinct parts A and B. Then a state $|\Psi\rangle$ of the whole system can be written as

$$|\Psi\rangle = \sum_{m,n} A_{m,n} |\Psi_m^A\rangle |\Psi_n^B\rangle, \tag{2.3}$$

where the $|\Psi_m^{A/B}\rangle$ are orthogonal basis functions for the distinct Hilbert spaces. From the singular-value decomposition (SVD) theorem we can write the rectangular coefficient matrix $\mathbf{A}$ as $\mathbf{UDV}$, where the matrices $\mathbf{U}, \mathbf{V}$ are unitary, and $\mathbf{D}$ is diagonal. If we transform the bases of subsystems A and B by $\mathbf{U}$ and $\mathbf{V}$ respectively. We get the Schmidt decomposition[**Peschel'2009**]

$$|\Psi\rangle = \sum_{n} \lambda_n |\Phi_n^A\rangle |\Phi_n^B\rangle, \tag{2.4}$$

where now we get the total wavefunction is given as sum of products of two orthogonal functions. The λ_n are the diagonal elements of $\mathbf{D}$ which for a normalised $|\Psi\rangle$ obey $\sum_i |\lambda_i|^2 = 1$. It is important to note that all entanglement information are encoded in the λ_n's like for a product state all except one λ_n is non-zero, or for a maximally entangled state all λ_n's are equal. The $|\lambda_n|^2$'s are known as the Schmidt coefficients and the number of non-zero Schmidt coefficients is called the Schmidt rank.

2.2.2 Entanglement Spectrum

The reduced density matrices (RDM) are given by $\rho_{\mathrm{A/B}} = \mathrm{Tr}_{\mathrm{B/A}}[\rho]$. So from eq(2.4) we get

$$\rho_{\mathrm{A/B}} = \sum_{n} |\lambda_n|^2 |\Phi_n^{\mathrm{A/B}}\rangle \langle \Phi_n^{\mathrm{A/B}}|. \tag{2.5}$$

It should be noted that both the RDM's (ρ_A and ρ_B) have the same eigenvalues given by $|\lambda_i|^2$. This eigenvalue spectrum of the reduced density matrix is known as the Entanglement Spectrum.

2.2.3 Entanglement Entropy

The n^{th} Renyi-entropy for the subsystem A is given as

$$S_{Renyi}^{(n)} = \frac{1}{1-n} \log \mathrm{Tr}_{\mathrm{A}}[\rho_A^n], \tag{2.6}$$

where ρ_A is the reduced density matrix for sub-system A. Similarly, the Von-Neumann entropy is given by

$$S_{VN} = -\mathrm{Tr}[\rho_A \ln \rho_A]. \tag{2.7}$$

In the limit $n \to 1$, we get (See Appendix A.1)

$$S_{VN} = \lim_{n \to 1} S^{(n)}_{Renyi}. \tag{2.8}$$

For non-interacting systems

$$S^{(n)}_{Renyi} = \frac{1}{1-n} \mathrm{Tr}[\ln[(1-C)^n + C^n]]. \tag{2.9}$$

and

$$S_{VN} = -\mathrm{Tr}[(1-\mathrm{C})\ln(1-\mathrm{C}) + (\mathrm{C})\ln(\mathrm{C})]. \tag{2.10}$$

where C is a $N_a \times N_a$ correlation matrix (See appendix A.2).

2.3 Correlation matrix

For a free-fermion system, consider the general non-interacting Hamiltonian

$$H = \sum_{i,j} h_{ij} c_i^\dagger c_j, \tag{2.11}$$

where $c_i^\dagger$ and c_i are the fermion creation and annhilation operator at site i respectively. We divide the system into two parts- subsystem A from $i = 1$ to $i = N_A$, and subsytem B from $i = N_A + 1$ to $i = N$. The one-particle correlation function is given as

$$C_{ij} = \mathrm{Tr}[\rho c_i^\dagger c_j] = \langle c_i^\dagger c_j \rangle = \langle \Psi | c_i^\dagger c_j | \Psi \rangle. \tag{2.12}$$

The correlation matrix element for the RDM of subsystem A is given as

$$C^A_{ij} = \mathrm{Tr_A}[\rho_A c_i^\dagger c_j] = \mathrm{Tr_A}[\mathrm{Tr_B}[\rho] c_i^\dagger c_j] = \mathrm{Tr_A}[\mathrm{Tr_B}[\rho \mathrm{c_i^\dagger c_j}]] = \mathrm{Tr}[\rho c_i^\dagger c_j], \tag{2.13}$$

where $i, j \in A$. So $C^A_{ij} = [C_{ij}]_{i,j \in A}$.

3. SSH Model

The Su-Schrieffer-Heeger model, also known as the SSH model, was first introduced to understand polyacetylene[**PhysRevLett.42.1698**] in 1979. Since then, it has come a long way and been experimentally realized in cold atomic systems[**Atala˙2013**].

3.1 Hamiltonian

The Hamiltonian for one-dimensional (1D) SSH model in second quantized notation is given as,

$$H = \sum_i \left[t_1 (a_i^\dagger b_i + b_i^\dagger a_i) + t_2 (a_{i+1}^\dagger b_i + b_i^\dagger a_{i+1}) \right] \tag{3.1}$$

where a_i and b_i destroys a fermion on site-i of sublattice-A and B respectively and t_1, t_2 are the intercell and intracell hopping parameters. For $|t_1| < |t_2|$ the system is a topological insulator (TI), $|t_1| > |t_2|$ the system is a non-TI and for $|t_1| = |t_2|$ there is a quantum critical point (QCP).

3.2 Correlation matrix for the thermal state

For the Hamiltonian in eq(2.11) we can diagonalize the matrix h_{ij} of the full system as

$$h = UDU^\dagger, \tag{3.2}$$

where U is a unitary matrix and D the diagonal matrix. Let E_i's be the diagonal entries (eigenvalues of h) of D. Then the hamiltonian can be rewritten as

$$H = \sum_k E_k (\sum_i U_{ik} c_i^\dagger)(\sum_j U_{jk}^\dagger c_j). \tag{3.3}$$

Transforming operator basis by introducing new operators

$$\tilde{c}_k = \sum_i U_{ik}^\dagger c_i \quad \text{and,} \quad \tilde{c}_k^\dagger = \sum_i U_{ik} c_i^\dagger. \tag{3.4}$$

The hamiltonian reduces to

$$H = \sum_k E_k \tilde{c}_k^\dagger \tilde{c}_k. \tag{3.5}$$

By using eq(2.12), the correlation matrix element can now be rewritten as

$$C_{ij} = \sum_{k=1}^{N} U_{ki}^\dagger U_{jk} \langle \Psi | \tilde{c}_k^\dagger \tilde{c}_k | \Psi \rangle. \tag{3.6}$$

For the thermal state of a free fermionic system, the expectation value of number of particles in state k is just the Fermi-Dirac distribution with energy E_k. Hence, the correlation matrix element becomes

$$C_{ij} = \sum_{k=1}^{N} U_{ki}^\dagger U_{jk} \frac{1}{e^{\beta E_k} + 1}. \tag{3.7}$$

3.3 Time evolving correlation matrix for a pure state

The time-evolving correlation matrix element can be written in Schrodinger or Heisenberg formulation as:

$$C_{ij}(t) \equiv \langle \psi(t) | c_i^\dagger c_j | \psi(t) \rangle = \langle \psi_0 | c_i^\dagger(t) c_j(t) | \psi_0 \rangle \tag{3.8}$$

where $\psi_0 = \psi(t=0)$ and $|\psi(t)\rangle = e^{-iHt}|\psi_0\rangle$. Writing the operator evolution in Heisenberg notation in the hamiltonian diagonal basis we get,

$$c_j(t) = e^{iHt}(\sum_\alpha U_{j\alpha}^\dagger \tilde{c}_\alpha) e^{-iHt} = \sum_\alpha e^{iE_\alpha t \tilde{c}_\alpha^\dagger \tilde{c}_\alpha} (U_{j\alpha}^\dagger \tilde{c}_\alpha) e^{-iE_\alpha t \tilde{c}_\alpha^\dagger \tilde{c}_\alpha} \tag{3.9}$$

Rest all the terms easily commute and cancel out. Now we use the below identity which is easy to prove using simple operator expansion and commutation of terms.

$$c e^{ac^\dagger c} = e^{a(1-c^\dagger c)} c \tag{3.10}$$

$$\implies c_j(t) = \sum_\alpha e^{iE_\alpha t \tilde{c}_\alpha^\dagger \tilde{c}_\alpha} U_{j\alpha}^\dagger e^{-iE_\alpha t(1-\tilde{c}_\alpha^\dagger \tilde{c}_\alpha)} \tilde{c}_\alpha \tag{3.11}$$

$$\implies c_j(t) = \sum_\alpha U_{j\alpha}^\dagger \tilde{c}_\alpha e^{-iE_\alpha t} \tag{3.12}$$

$$\implies C_{ij}(t) = \langle \psi_0 | [\sum_\beta U_{i\beta} \tilde{c}_\beta^\dagger e^{iE_\beta t}][\sum_\alpha U_{j\alpha}^\dagger \tilde{c}_\alpha e^{-iE_\alpha t}] | \psi_0 \rangle \tag{3.13}$$

$$\implies C_{ij}(t) = \sum_{\alpha\beta} U_{i\beta} U_{j\alpha}^\dagger e^{i(E_\beta - E_\alpha)t} \langle \psi_0 | \tilde{c}_\beta^\dagger \tilde{c}_\alpha | \psi_0 \rangle \tag{3.14}$$

Now the last term in the summation can be simplified by taking the operators to their

previous basis.

$$\langle\psi_0|\tilde{c}_\beta^\dagger\tilde{c}_\alpha|\psi_0\rangle = \langle\psi_0|(\sum_k U_{k\beta}c_k^\dagger)(\sum_{k'} U_{k'\alpha}^\dagger c_{k'})|\psi_0\rangle \tag{3.15}$$

$$\implies \langle\psi_0|\tilde{c}_\beta^\dagger\tilde{c}_\alpha|\psi_0\rangle = \sum_{k,k'} U_{k\beta}U_{k'\alpha}^\dagger\langle\psi_0|c_k^\dagger c_{k'}|\psi_0\rangle \tag{3.16}$$

$|\psi_0\rangle$ is the pure state at time t=0, given by

$$|\psi_0\rangle = |n_1 n_2 n_3 ...\rangle, \tag{3.17}$$

where the n_i's are either 0 or 1. Hence eq(3.15) simplifies to

$$\langle\psi_0|\tilde{c}_\beta^\dagger\tilde{c}_\alpha|\psi_0\rangle = \sum_{k,k'} U_{k\beta}U_{k'\alpha}^\dagger\delta_{k,k'}n_k = \sum_k U_{k\beta}U_{k\alpha}^\dagger n_k. \tag{3.18}$$

Now putting the above expression in eq(3.14)

$$\implies C_{ij}(t) = \sum_{\alpha\beta} U_{i\beta}U_{j\alpha}^\dagger e^{i(E_\beta - E_\alpha)t}(\sum_k U_{k\beta}U_{k\alpha}^\dagger n_k) \tag{3.19}$$

$$\implies C_{ij}(t) = \sum_{\alpha\beta k} U_{i\beta}U_{j\alpha}^\dagger U_{k\beta}U_{k\alpha}^\dagger n_k e^{i(E_\beta - E_\alpha)t}. \tag{3.20}$$

Computation of correlation matrix: Now when one tries to find the correlation matrix at each point of time, we have to go through a total of 5 nested loops (i, j, k, α, β) which makes it almost impossible to do the calculations for N = 100 or 200 sites. We use the idea of vectorization (parallel computing), which reduces the time taken to run the code from days to seconds. Instead of going through nested loops, we convert the loops to matrices that allow us to do multiple parallel computations simultaneously.

4. Results

4.1 Entropy vs Subsystem size

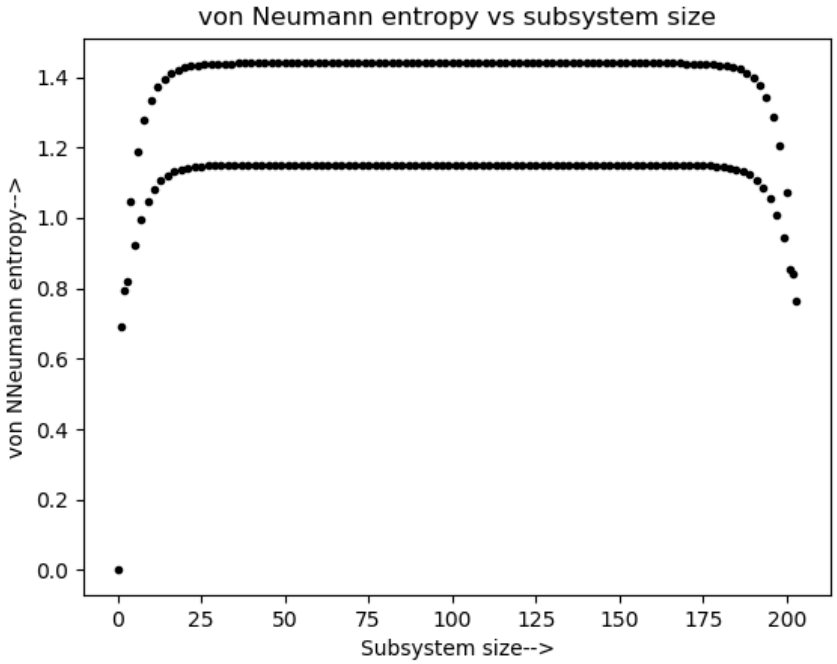

Figure 4.1: von Neumann entropy vs Subsystem size for $T = 0$ for periodic boundary condition (PBC) SSH model with N=204 sites, and hopping parameters t_1=0.8 and t_2=1. The quantity oscillates between two values S_1 and S_2, whether subsytem size is odd or even. S_2=1.4186 and S_2=0.9486.

The von Neumann entropy is almost constant for each of the odd and even subsystem sizes (l) and follows the area law. If a state satisfies area law then the leading term in entanglement entropy grows proportionally with the boundary of the partition. For 1D systems the boundaries become zero dimensional, which we see from the graph. The entropy gives two oscillatory values-

$$S(l) = S_1 \quad \text{if } l \bmod 2 = 1$$
$$S_2 \quad \text{if } l \bmod 2 = 0.$$

The difference between S_2 and S_1, ΔS changes sign when one goes from topologi-

cal to trivial. One can introduce a characterization of topological order based on bulk oscillations of entanglement entropy [**PhysRevB.101.235155**].

4.2 Entropy vs Temperature

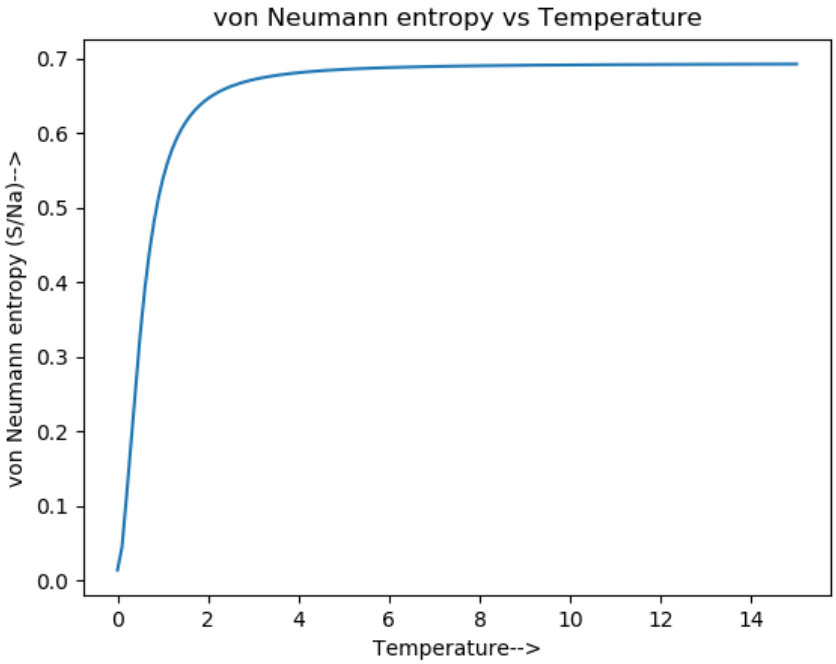

Figure 4.2: Bipartite von Neumann entropy persite vs temperature for the thermal state with free boundary conditions (FBC) of the SSH model with N=204 sites, hopping parameters t_1=0.8 and t_2=1, T_{min}=0, T_{max}=15 and N_{temp}(Number of temperature points)=150.

The formula used for calculating the bipartite von Neumann entropy is eq(3.20). There are a few essential points to be noted -
1) The entropy looks like zero at $T = 0$, which is not true because we have some entropy of entanglement even at zero temperatures.
2) The entropy per site for a thermal state at high temperature is $ln(2)$ as we would expect because at high temperatures entropy becomes extensive and only depends on the filling factor.
3) The change of boundary condition from FBC to PBC barely changes the graph.
4) The same happens for the second Renyi entropy.

4.3 Time evolution of entropy

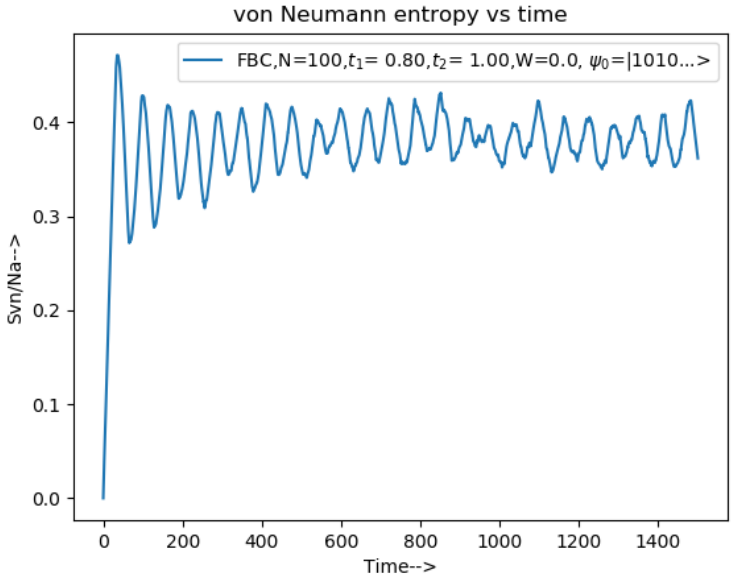

Figure 4.3: Bipartite von Neumann entropy persite vs time for a time evolving FBC density wave like pure state of the SSH model with N=100 sites, hopping parameters t_1=0.8 and t_2=1, t_{min}=0, t_{max}=1500 and N_{time}(Number of time points)=6000.

We get the time-evolving correlation matrix formula from eq(3.33) and use eq(2.10) to get the entanglement entropy at each instant of time. We suspect that oscillations in the entropy are due to Poincare recurrence.

4.3.1 Different pure states

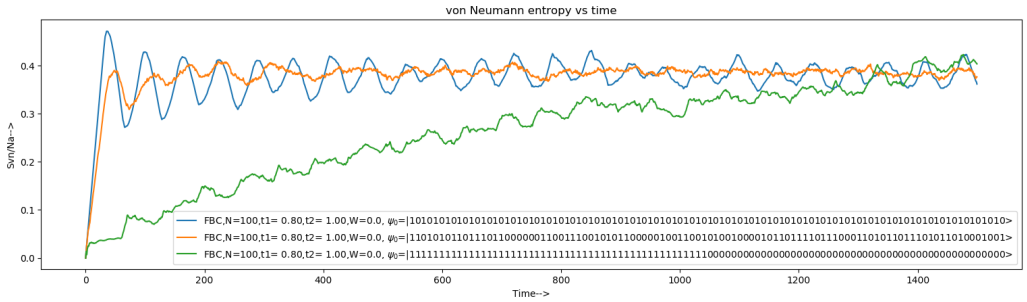

Figure 4.4: Bipartite von Neumann entropy persite vs time for time evolving FBC pure states - density wave like state (shown in blue), random half-filled state (shown in orange), first half filled and next half empty state (shown in green) of the SSH model with N=100 sites, hopping parameters t_1=0.8 and t_2=1, t_{min}=0, t_{max}=1500 and N_{time}= 6000.

We observe that the random state does not fluctuate much from the asymptotic entropy value, whereas the fluctuations are high in the density wave like state. The third pure

state takes a much larger time to start fluctuating around the asymptotic entropy value.

4.3.2 Phase transition

The phase transition criteria as written in Sec 3.1 is as follows:
1) For $|t_1| < |t_2|$ the system is a topological insulator (TI).
2) For $|t_1| > |t_2|$ the system is topologically trivial
3) For $|t_1| = |t_2|$ there is a quantum critical point (QCP).

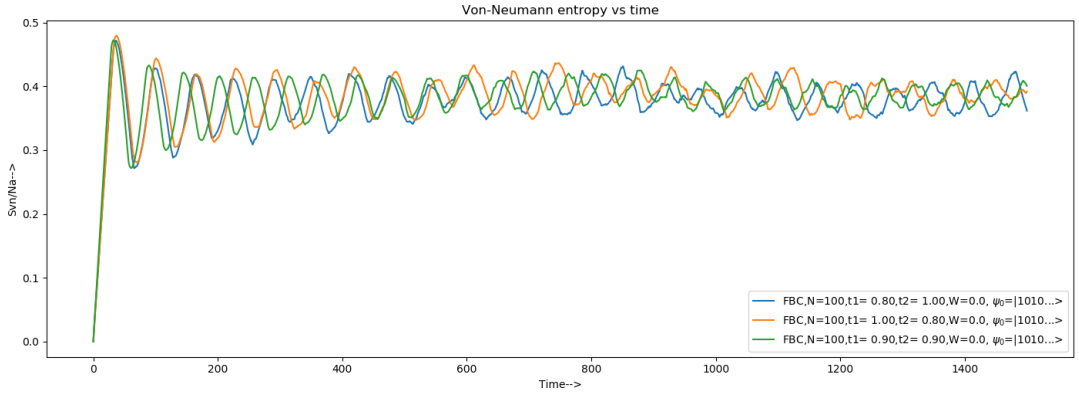

Figure 4.5: Bipartite von Neumann entropy persite vs time for a time evolving FBC density wave like pure state of the SSH model with N=100 sites, three set of hopping parameters (t_1, t_2)=(0.8,1);(1,0.8);(0.9,0.9); t_{min}=0, t_{min}=0, t_{max}=1500 and N_{time}=6000.

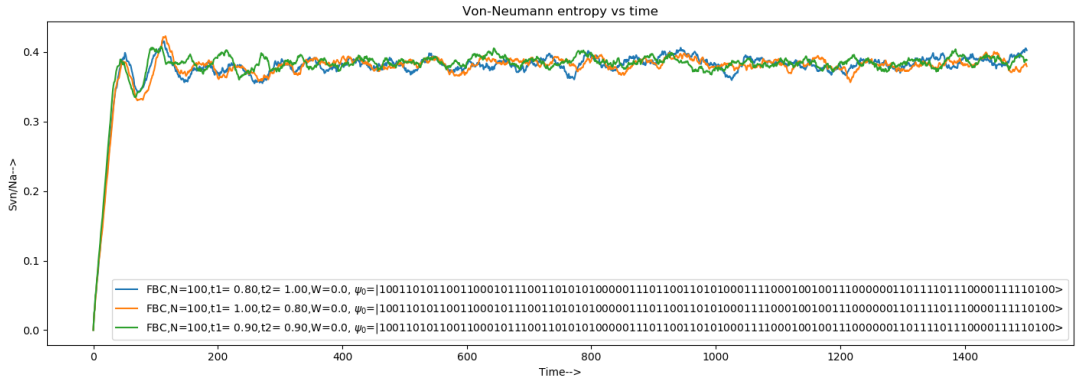

Figure 4.6: Bipartite von Neumann entropy persite vs time for a time evolving FBC random half filled pure state of the SSH model with N=100 sites, three set of hopping parameters (t_1, t_2)=(0.8,1);(1,0.8);(0.9,0.9); t_{min}=0, t_{max}=1500 and N_{time}=6000.

4.3.3 Effect of system size

For the number of sites less than 50, we get a jittery graph from which one cannot see oscillations in entropy as time increases. For 100 and more sites, this oscillation becomes

clear. We see the effect of increasing system size and how it affects the entropy per site vs. time graphs below.

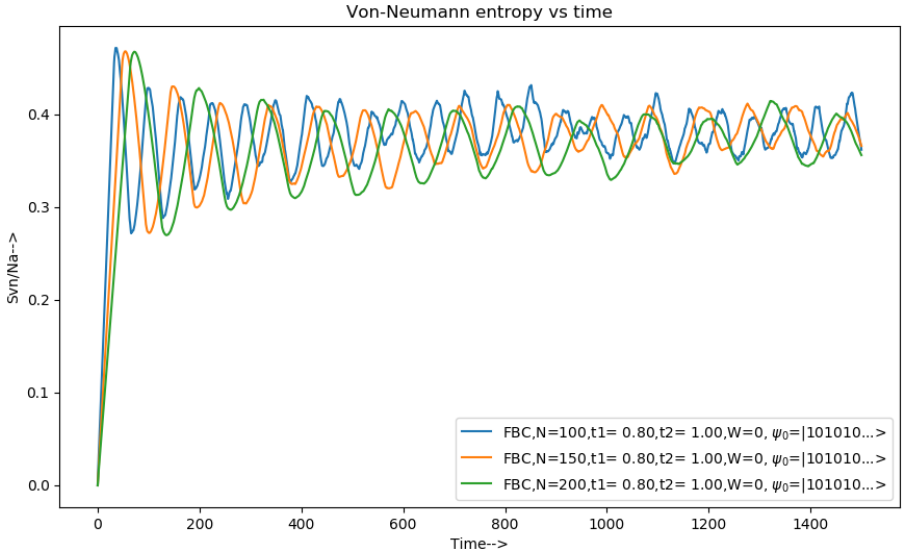

Figure 4.7: Bipartite von Neumann entropy persite vs time for a time evolving FBC density wave like pure state of the SSH model with N=100, 150, 200 sites, hopping parameters t_1=0.8 and t_2=1, t_{min}=0, t_{max}=1500 and N_{time}=6000.

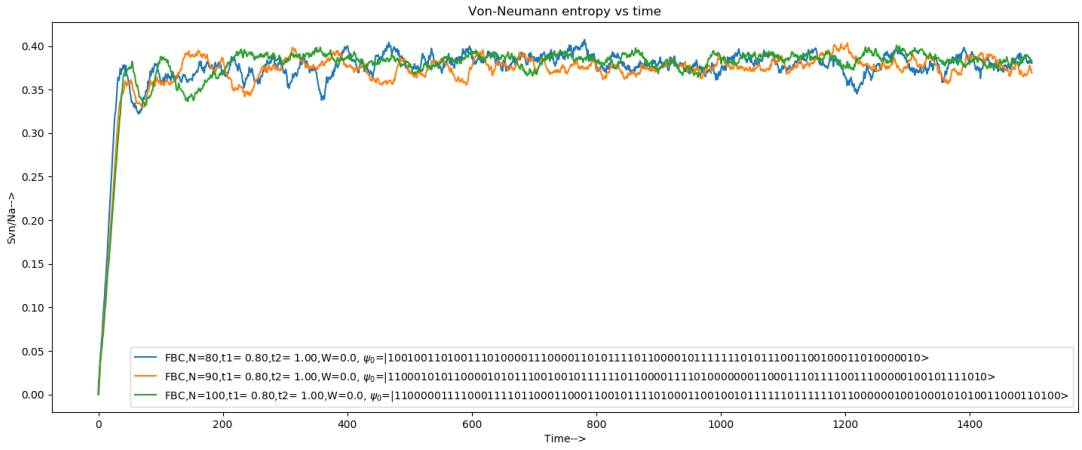

Figure 4.8: Bipartite von Neumann entropy persite vs time for a time evolving FBC random half filled pure state of the SSH model with N=80, 90, 100 sites, hopping parameters t_1=0.8 and t_2=1, t_{min}=0, t_{max}=1500 and N_{time}=6000.

4.3.4 Effect of boundary conditions

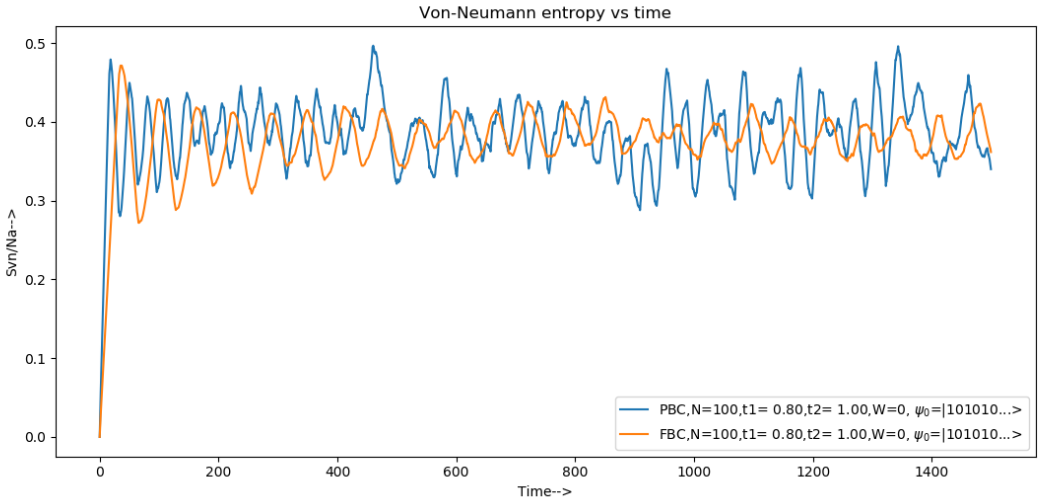

Figure 4.9: Bipartite von Neumann entropy persite vs time for a time evolving FBC and PBC, density wave like pure state of the SSH model with N=100 sites, hopping parameters t_1=0.8 and t_2=1, t_{min}=0, t_{max}=1500 and N_{time}=6000.

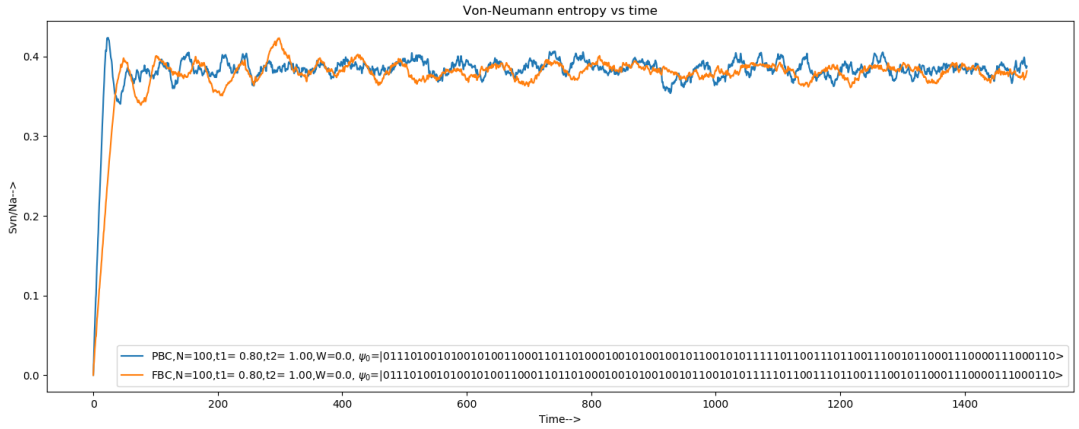

Figure 4.10: Bipartite von Neumann entropy persite vs time for a time evolving FBC and PBC, random half-filled pure state of the SSH model with N=100 sites, hopping parameters t_1=0.8 and t_2=1, t_{min}=0, t_{max}=1500 and N_{time}=6000.

We can see the effect of changing boundary conditions from PBC to FBC in the above graph. At short times both of them behave almost identically, but after that, they separate and behave differently.

4.3.5 Effect of disorder

We can see the effect of random onsite disorder in the Hamiltonian as

$$H = \sum_i \left[t_1(a_i^\dagger b_i + b_i^\dagger a_i) + t_2(a_{i+1}^\dagger b_i + b_i^\dagger a_{i+1}) + w_i a_i^\dagger a_i + w_i' b_i^\dagger b_i \right] \tag{4.21}$$

where $w_i, w_i' \in [-W, W]$ are the random on-site disorder for A and B sublattice respectively. On adding slight disorder we observe from the graph below that the disorder reduces the asymptotic value of the entropy per site.

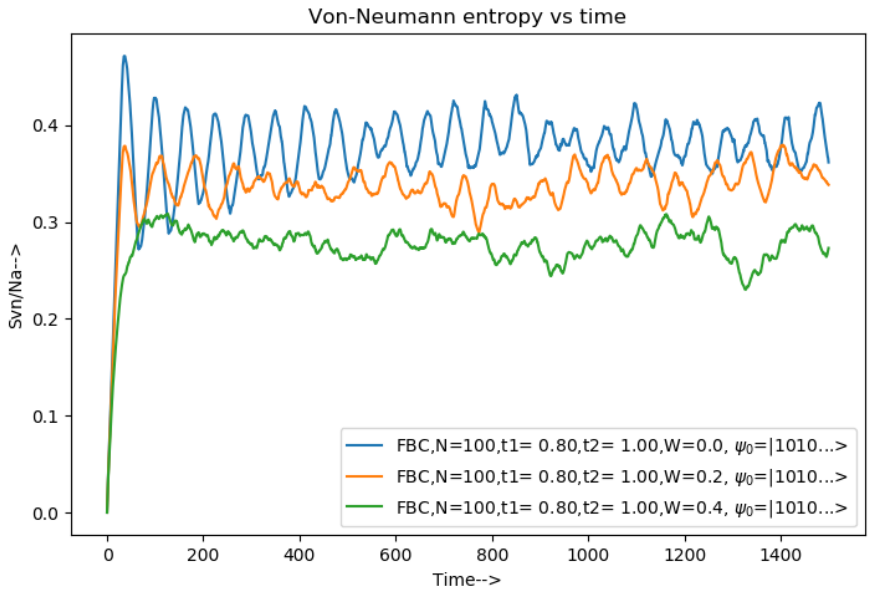

Figure 4.11: Bipartite von Neumann entropy persite vs time for a time evolving FBC density wave like pure state of the SSH model with N=100 sites, hopping parameters t_1=0.8 and t_2=1, disorder parameter values W=0, 0.2, 0.4; t_{min}=0, t_{max}=1500 and N_{time}=6000.

5. Conclusions and Future work

The signatures of symmetry-protected topology are not quite distinguishable - as one might see from fig.(4.5) and fig.(4.6). One also finds from fig.(4.1) and fig.(4.3) that the entanglement entropy of the ground state is 1-order of magnitude smaller than that of the pure states that we considered. Hence to observe the changes in entanglement entropy due to topological transition properly, one has to go to the low energy states. The changes in boundary conditions do not give a distinguishable change in entanglement entropy. Changing the system size still gives around the same asymptotic entropy value, which in a way implies that the system has thermalized, so the entropy is extensive. Since the system is 1D, we know that any amount of disorder will cause Anderson localization. This causes the electrons to localize in a space (order of localization length), leading to a decrement in entanglement entropy.

This subsection explores in some detail the future direction of this research-
1) Taking low energy states and looking at their time evolution with phase transitions.
2) Even though the system is a non-interacting model, will it approximately thermalize?
3) Looking into other similar models like the Kitaev chain.

Part I

Appendix A

Calculations

A.1 Relation between von Neumann entropy and Renyi entropy

In the limit n $\to$ 1, we have

$$S^{(1)}_{Renyi} = \lim_{n\to 1} \frac{\log \mathrm{Tr_A}[\rho_A^n]}{1-n} = \lim_{n\to 1} \frac{\mathrm{Tr_A}[\rho_A^n] - 1}{1-n} = -\frac{\partial}{\partial n} \log \mathrm{Tr_A}[\rho_A^n]\Big|_{n=1} \tag{A.1}$$

For the last equality we have used the replica trick. Let λ_i be the eigenvalues of ρ_A, then

$$\log \mathrm{Tr_A}[\rho_A^n] = \log\Big(\sum_i \lambda_i^n\Big). \tag{A.2}$$

$$\implies -\frac{\partial}{\partial n} \log \mathrm{Tr_A}[\rho_A^n]|_{n=1} = -\frac{\sum_i \lambda_i^n \log\lambda_i}{\sum_i \lambda_i^n}\Big|_{n=1} = -\frac{\sum_i \lambda_i \log\lambda_i}{\sum_i \lambda_i^n} \tag{A.3}$$

Since, $\mathrm{tr_A}\rho_A = 1$, this implies that $\sum_i \lambda_i = 1$.

$$\implies -\frac{\partial}{\partial n} \log \mathrm{Tr_A}[\rho_A^n]|_{n=1} = -\sum_i \lambda_i \log\lambda_i = -\mathrm{Tr}[\rho_A \ln \rho_A] \tag{A.4}$$

Hence,

$$S_{VN} = \lim_{n\to 1} S^{(n)}_{Renyi}. \tag{A.5}$$

A.2 Relation between Entanglement Entropy and Correlation Matrix for non-interacting systems

Since ρ_A is Hermitian and positive semidefinite. We can take ρ_A of the form of

$$\rho_A = \frac{e^{-H^A}}{Z} \tag{A.6}$$

The Hamiltonian H^A is known as the entanglement Hamiltonian. We do as done in Sec. (3.2) just instead of summing over the whole system; we now sum over the subsystem A. Doing that will give us an equation exactly like eq(3.7). That equation shows that if ϵ_i are the eigenvalues of the Hamiltonian (H^A), then eigenvalues of the correlation matrix are

$$\lambda_i = \frac{1}{1+e^{\epsilon_i}}. \tag{A.7}$$

We first calculate the below expression which will further simplify our calculations.

$$\mathcal{Z} = \mathrm{tr}(e^{-mH^A}) \tag{A.8}$$

$$\implies \mathcal{Z} = \mathrm{tr}(e^{-m\sum_k \epsilon_k a_k^\dagger a_k}) = \sum_{n_k} \langle n_1 n_2 ... n_{N_A} | e^{-m\sum_k \epsilon_k a_k^\dagger a_k} | n_1 n_2 ... n_{N_A} \rangle = \Pi_n (1+e^{-m\epsilon_n}). \tag{A.9}$$

Let's first simplify eq(2.6),

$$S^{(n)}_{Renyi} = \frac{1}{1-n}\log \mathrm{Tr_A}[\rho_A^n] = \frac{1}{1-n}\log \mathrm{Tr_A}[e^{-nH^A}/Z^n] = \frac{1}{1-n}\log\left[\frac{\mathrm{Tr_A}[e^{-nH^A}]}{Z^n}\right] \tag{A.10}$$

$$\implies S^{(n)}_{Renyi} = \frac{1}{1-n}\log\left[\frac{\Pi_k(1+e^{-n\epsilon_k})}{\Pi_k(1+e^{-\epsilon_k})^n}\right] = \frac{1}{1-n}\log\left[\frac{\Pi_k(e^{n\epsilon_k}+1)}{\Pi_k(e^{\epsilon_k}+1)^n}\right] \tag{A.11}$$

$$\implies S^{(n)}_{Renyi} = \frac{1}{1-n}\sum_k \log\left[\frac{(e^{n\epsilon_k}+1)}{(e^{\epsilon_k}+1)^n}\right] = \frac{1}{1-n}\sum_k \log\left[\frac{e^{n\epsilon_k}}{(e^{\epsilon_k}+1)^n} + \frac{1}{(e^{\epsilon_k}+1)^n}\right] \tag{A.12}$$

Using eq(A.7) we get

$$\implies S^{(n)}_{Renyi} = \frac{1}{1-n}\sum_k \log[\lambda_k^n + (1-\lambda_k)^n]. \tag{A.13}$$

Now we simplify eq(2.9) for that we use the standard trace log relation that $log(det(A)) = tr(log(A))$. This reduces the problem to finding the eigenvalues of - $C^n + (1-C)^n$.

$$S^n_A = \frac{1}{1-n}\mathrm{tr}[\ln[(1-C)^n + C^n]] = \frac{1}{1-n}\ln[\det[(1-C)^n + C^n]]. \tag{A.14}$$

Note that the matrices C^n and $(1-C)^n$ commute and have eigenvalues λ_i^n and $(1-\lambda_i)^n$ respectively. This implies that the eigenvalues of $C^n + (1-C)^n$ are just $\lambda_i^n + (1-\lambda_i)^n$.

$$\implies S^n_A = \frac{1}{1-n}\ln[\ \Pi_i(\lambda_i^n + (1-\lambda_i)^n)] = \frac{1}{1-n}\sum_k \log[\lambda_k^n + (1-\lambda_k)^n]. \tag{A.15}$$

$$\implies S^{(n)}_{Renyi} = \frac{1}{1-n}\log \mathrm{Tr_A}[\rho_A^n] = \frac{1}{1-n}\mathrm{tr}[\ln[(1-C)^n + C^n]]. \tag{A.16}$$

Part II

Appendix B

Python codes

B.1 Defining useful functions

a

B.2 Entropy vs Subsytem size

B.3 Entropy vs Temperature

B.4 Entropy vs Time

a